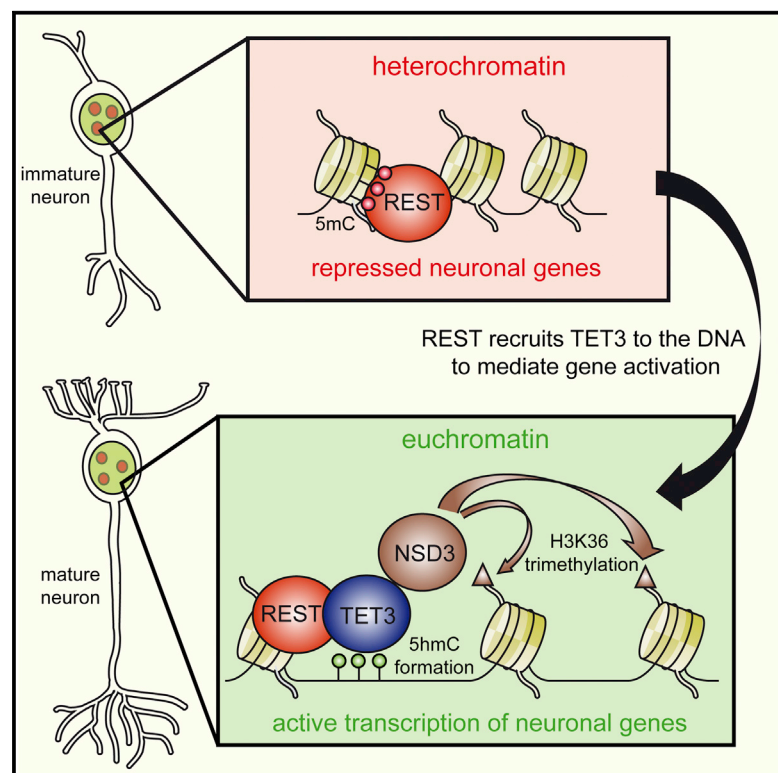


TET3 Is Recruited by REST for Context-Specific Hydroxymethylation and Induction of Gene Expression

Graphical Abstract



Authors

Arshan Perera, David Eisen, ..., Thomas Carell, Stylianos Michalakis

Correspondence

thomas.carell@cup.uni-muenchen.de (T.C.),
stylianos.michalakis@cup.uni-muenchen.de (S.M.)

In Brief

Neuronal differentiation involves major epigenetic changes, such as accumulation of 5-hydroxymethylcytosine (5hmC). Perera et al. found that TET3 interacts with transcriptional regulators and histone writers. They demonstrate that REST recruits TET3 for context-specific 5hmC formation and TET3 recruits NSD3 for H3K36 trimethylation.

Highlights

- TET3 interacts with transcriptional regulators and histone writers
- REST recruits TET3 and stimulates its hydroxylase activity
- TET3 activates context-specific gene transcription
- TET3 enhances the activity of NSD3 to generate H3K36 trimethylation

Accession Numbers

GSE65860
PXD001857



TET3 Is Recruited by REST for Context-Specific Hydroxymethylation and Induction of Gene Expression

Arshan Perera,^{1,3} David Eisen,^{2,3} Mirko Wagner,^{2,3} Silvia K. Laube,² Andrea F. Künzel,² Susanne Koch,¹ Jessica Steinbacher,² Elisabeth Schulze,¹ Victoria Splith,¹ Nana Mittermeier,¹ Markus Müller,² Martin Biel,¹ Thomas Carell,^{2,*} and Stylianos Michalakis^{1,*}

¹Center for Integrated Protein Science Munich CiPSM at the Department of Pharmacy – Center for Drug Research, Ludwig-Maximilians-Universität München, 81377 Munich, Germany

²Center for Integrated Protein Science Munich CiPSM at the Department of Chemistry, Ludwig-Maximilians-Universität München, 81377 Munich, Germany

³Co-first author

*Correspondence: thomas.carell@cup.uni-muenchen.de (T.C.), stylianos.michalakis@cup.uni-muenchen.de (S.M.)

<http://dx.doi.org/10.1016/j.celrep.2015.03.020>

This is an open access article under the CC BY-NC-ND license (<http://creativecommons.org/licenses/by-nc-nd/4.0/>).

SUMMARY

Ten-eleven translocation hydroxylases (TET1-3) oxidize 5-methylcytosine (5mC) to 5-hydroxymethylcytosine (5hmC). In neurons, increased 5hmC levels within gene bodies correlate positively with gene expression. The mechanisms controlling TET activity and 5hmC levels are poorly understood. In particular, it is not known how the neuronal TET3 isoform lacking a DNA-binding domain is targeted to the DNA. To identify factors binding to TET3, we screened for proteins that co-precipitate with TET3 from mouse retina and identified the transcriptional repressor REST as a highly enriched TET3-specific interactor. REST was able to enhance TET3 hydroxylase activity after co-expression and overexpression of TET3-activated transcription of REST target genes. Moreover, we found that TET3 also interacts with NSD3 and two other H3K36 methyltransferases and is able to induce H3K36 trimethylation. We propose a mechanism for transcriptional activation in neurons that involves REST-guided targeting of TET3 to the DNA for directed 5hmC generation and NSD3-mediated H3K36 trimethylation.

INTRODUCTION

Epigenetic mechanisms are critically involved in neuronal differentiation and synaptic network formation. 5-hydroxymethylcytosine (5hmC), a recently identified epigenetic DNA modification, is present at high levels in the brain (Münzel et al., 2010) and accumulates during neuronal differentiation (Hahn et al., 2013). 5hmC is generated by ten-eleven translocation (TET) hydroxylases (TET1-3) from 5-methylcytosine (5mC) (Kriaucionis and Heintz, 2009; Tahiliani et al., 2009). Accumulation of 5hmC in neuronal genes was shown to correlate positively with gene expression (Colquitt et al., 2013; Hahn et al., 2013; Mellén et al., 2012; Song et al., 2011; Szulwach et al.,

2011), suggesting that 5hmC plays a key role in neuronal differentiation (Santiago et al., 2014). How TET hydroxylase activity is controlled and directed to neuronal genes is not known. The TET1 isoform contains an amino-terminal CXXC domain that is thought to be important for binding to DNA (Xu et al., 2011). Tet2 lacks such a CXXC domain, but was shown to functionally interact with the CXXC domain containing proteins CXXC4 and CXXC5 (Ko et al., 2013; Williams et al., 2011).

TET3, the major TET isoform in neurons (Colquitt et al., 2013; Hahn et al., 2013), exists in various isoforms generated by alternative splicing (Liu et al., 2013), two isoforms containing a CXXC domain and one shorter isoform lacking such a domain. In particular, the TET3 lacking a CXXC domain (neuronal TET3) was shown to be enriched in neuronal tissue (Liu et al., 2013). It is not known how neuronal TET3 is targeted to the DNA. It was suggested that transcriptional regulators might bind directly to TET3, facilitating its specific targeting to genomic positions, and, hence, control 5hmC levels (Xu et al., 2012). Transcription-factor-dependent control of TET3 activity could potentially contribute to epigenetic regulation of gene expression in neurons. However, transcriptional regulators that functionally interact with TET3 have not been identified so far.

To directly address this issue, we investigated the function of TET3 and 5hmC during the formation of a complex neural network: the murine retina. We show that 5hmC levels increase during postnatal retinal network maturation. This gain of 5hmC results in an elevated expression of genes involved in important retinal and/or neuronal functions. To identify factors able to regulate TET3 activity and 5hmC formation in a gene-specific manner, we purified retinal nuclear proteins interacting with TET3. We found that the transcriptional regulator REST specifically interacts with the neuronal TET3 isoform and elevates its hydroxylase activity. Moreover, we show that TET3 overexpression induces the expression of REST target genes. We postulate that transcriptional activation of specific genes results from de novo chromatin remodeling that involves activity of histone 3 lysine 36 methyltransferases like NSD3.

RESULTS

5hmC Is Acquired during Postnatal Retinal Development

Development of neural networks is a complex process that involves the generation, positioning, and synaptic wiring of neurons. This developmental process is finalized with activity-dependent maturation of neurons and refinement of their network. In the mammalian retina, this terminal maturation process involves major morphological and functional changes, largely occurring within a week after eye opening (Hoon et al., 2014; Okawa et al., 2014). These morphological and functional refinements go along with significant changes in the gene expression pattern. To visualize these changes, we applied label-free quantification (LFQ) comparing the retinal protein levels in 2-week-old mice (eye opening) with 3-week-old mice (mature state; Figure 1A), and we found a significant upregulation of proteins involved in synaptic function and visual processing over time (Figures 1A and S1A; Table S1). The molecular mechanisms controlling the underlying transcriptional changes are only partially understood (Gregory-Evans et al., 2013; Xiang, 2013).

We hypothesized that epigenetic regulation at the level of DNA might be involved. First evidence comes from the finding that the levels of the epigenetic DNA modification 5hmC in brain neurons increase with age (Hahn et al., 2013; Münzel et al., 2010). To test for its involvement in terminal retinal maturation, we analyzed the levels of 5hmC during this period. We first used a 5hmC-specific antibody for immunolocalization studies on retinal cryosections and observed a strong increase of the 5hmC immunosignal in all nuclear layers of the retina between week 2 and week 3 (Figures 1B and 1C). At eye opening (week 2), we observed high levels of 5hmC in nuclei of cells within the inner nuclear layer (INL) and the ganglion cell layer (GCL). In contrast, photoreceptor nuclei located in the outer nuclear layer (ONL) were immunonegative (Figure 1B). Strikingly, only 1 week after eye opening (week 3), the levels of 5hmC increased dramatically in both the INL and the GCL. Moreover, rod and cone photoreceptors in the ONL were now positive for 5hmC (Figures 1C and 1D). Confirming the specificity of the anti-5hmC antibody, the immunosignal was quantitatively depleted by 2.5 μ M 5hmC-containing DNA oligonucleotides (Figure 1C, inset). At the sub-nuclear level, most of the 5hmC signal was found to localize in euchromatic regions in both conventional and inverted nuclei (Figures 1E and 1F). In contrast, we found 5mC to be concentrated in pericentromeric heterochromatin (Figures 1E and 1F), suggesting that while 5mC is present in transcriptionally silenced regions, 5hmC is associated with transcriptional activity.

To quantify the levels of 5hmC along with all other cytosine modifications in mouse genomic DNA, we combined ultra-high-performance liquid chromatography with tandem mass spectrometry (UHPLC-MS/MS) (Schuesser et al., 2013; Table S7). The levels of 5hmC increased significantly (Figure 1G and S1B) ($p < 0.005$, Student's *t* test), whereas the levels of the further oxidized derivative 5-formylcytosine (5fC) dropped significantly during the same time frame (Figures 1I and S1C), suggesting distinct roles for 5hmC and 5fC in neurons. Interestingly, the levels of 5mC remained stable during this developmental window (Figures 1H and S1D).

Thus, retinal cells specifically accumulate genomic 5hmC levels during terminal retinal maturation. Importantly, retinal cells

at this developmental stage do not divide; thus, this effect cannot result from increased DNA replication.

To investigate the dynamics of 5hmC and 5mC formation in non-dividing cells, we performed an isotope-tracing experiment by culturing retinal explants from 11-day-old mice for 12 days in the presence of the labeled methyl group donor [$^{13}\text{CD}_3$]-methionine, which provides labeled 5mC (5- $^{13}\text{CD}_3$ -mC) and 5hmC (5- $^{13}\text{CD}_2$ -hmC) that can be quantified using UHPLC-MS/MS (Table S8). Confirming the presence of de novo methylation in terminally differentiated retinal cells, we detected 5- $^{13}\text{CD}_3$ -mC at linearly increasing levels (slope: 0.531, $R^2 = 0.999$) reaching a value of 3.9% of total 5mC after 9 days of [$^{13}\text{CD}_3$]-methionine feeding (Figure 1J). We further detected [$^{13}\text{CD}_2$]-labeled 5hmC (Figure 1K). However, the level of 5- $^{13}\text{CD}_2$ -hmC was low with only up to 1.6% after 9 days (slope: 0.208, $R^2 = 0.997$). Moreover, the majority of de novo 5hmC was generated from pre-existing and hence unlabeled 5mC (Figure S1E).

5hmC Accumulates in Neuronal Genes and Leads to Increased Gene Expression

To assess the genomic distribution of 5hmC during retinal maturation, we performed antibody-based 5hmC DNA immunoprecipitation (hMeDIP) from 2- and 3-week-old retina followed by next-generation sequencing (NGS). In agreement with the immunohistochemical and UHPLC-MS/MS quantification data, we identified 5,921 intragenic regions that gained 5hmC signal and approximately 20 times less with lost 5hmC signal (Figures 2A and S2A; Table S9). Gene ontology (GO) analysis revealed that genes involved in the morphology of nervous system, CNS development, differentiation of neurons, neuritogenesis, or guidance of axons are significantly enriched within the group of genes that gained 5hmC after eye opening (from week 2 to week 3) (Figure 2B). The genes enriched in the hMeDIP analysis were positively correlated to those enriched in the group of proteins with elevated expression in the mature retina ($p = 6.2 \times 10^{-11}$, Fischer's exact test; Figures 1A and S2B; Table S1). Moreover, 5hmC marks were particularly enriched in gene bodies (Figure 2C), suggesting a regulatory function of 5hmC in gene expression. To investigate if gain of 5hmC is associated with active transcription, we correlated the hMeDIP data with the LFQ protein expression data and found that gain of 5hmC levels from week 2 to week 3 resulted in significantly increased protein expression of the corresponding genes (Figure 2D).

Neuronal TET3 Interacts with Transcriptional Regulators and Histone Writers

5hmC is generated from 5mC by TET hydroxylases. To study if the elevated 5hmC levels in the mature retina result from increased TET-mediated oxidation, we analyzed the expression profile of the three TET enzymes during postnatal development of the mouse retina. We first found that TET3 is the dominant isoform in the retina and its levels increase at eye opening (Figure 3A; Table S10). Importantly, the expression levels at eye opening (postnatal day 13, p13) and at the mature stage (p20) were comparable, ruling out that increased Tet expression causes the increased 5hmC levels (Figure 3A).

TET3 exists in three isoforms that differ in their N-terminal sequence: two isoforms with a CXXC DNA-binding domain and

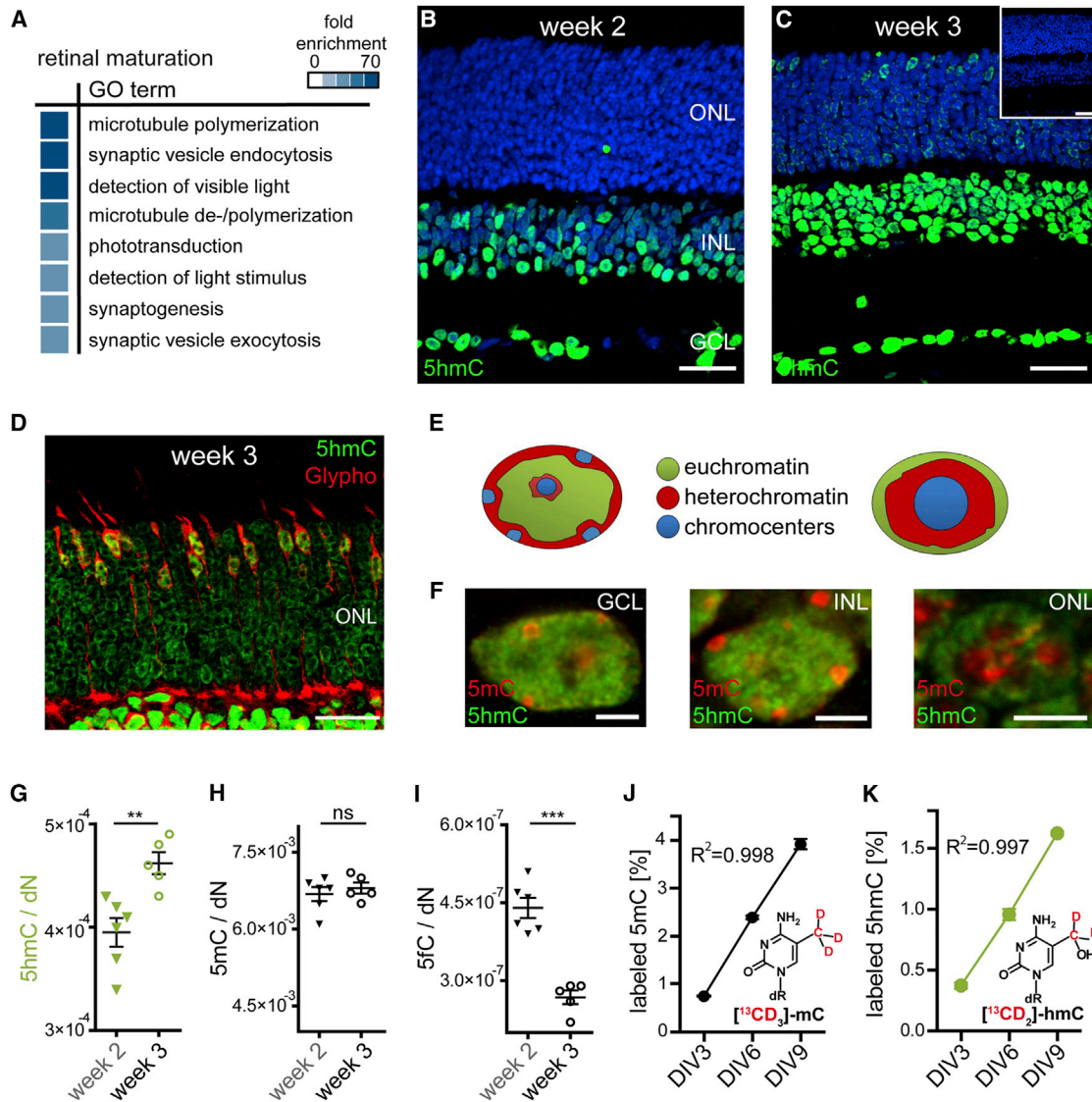


Figure 1. Transcriptional and Epigenetic Changes during Retinal Maturation

(A) GO analysis of upregulated proteins during retinal maturation (from eye opening at week 2 to terminal maturation of the retina at week 3) identified by LFQ is shown.

(B and C) Confocal scans from mouse retinal slices at week 2 (B) and week 3 (C) immunolabeled for 5hmC (green). There is a marked increase in 5hmC signal in nuclei of all retinal layers from week 2 to week 3, in particular in photoreceptors (ONL). The inset in (C) is from a depletion experiment proving the specificity of the anti-5hmC antibody.

(D) Magnification of ONL stained for 5hmC (green) and glycogen phosphorylase (Glypho) (red) is shown.

(E) Schematic view of conventional and inverted nuclei depicts heterochromatin and euchromatin regions.

(F) High-magnification images of conventional nuclei within the GCL or the INL and a rod nucleus with inverted nuclear architecture (Solovei et al., 2009) co-immunolabeled with 5hmC (green) and 5mC (red). In all cases, 5hmC is mainly found in euchromatin whereas 5mC is localized in heterochromatic regions.

(G–I) Scatter plots of UHPLC-MS/MS quantification of global (G) 5hmC, (H) 5mC, and (I) 5fC in the mouse retina at weeks 2 and 3 reveal an age-dependent increase in 5hmC levels, stable 5mC levels, and decreasing 5fC levels.

(J and K) Isotope tracing combined with UHPLC-MS/MS in mouse retinal explant cultures. Retinal explant cultures were fed with [methyl-¹³CD₃]-L-methionine and harvested for UHPLC-MS/MS quantification of labeled 5mC (J) and 5hmC (K) after 3, 6, and 9 days in vitro (DIV). Summary data are mean ± SEM in (G–I) and mean ± SD in (J and K). **p < 0.01, ***p < 0.001 (Student's t test). The cell nuclei in (A and B) were stained with Hoechst 3442 nuclear dye (blue). Scale bar, 25 μm in (B–D) and 3 μm in (F). See also Figure S1 and Tables S7 and S8.

a short isoform enriched in neuronal cells lacking the CXXC domain (Liu et al., 2013). Using isoform-specific primer sets, we found that the short variant lacking the CXXC domain is the

major TET3 isoform in the retina (Figure 3B). Other than the isoforms with the CXXC domain, this neuronal TET3 variant has no DNA-binding affinity (Xu et al., 2012). We hypothesized that

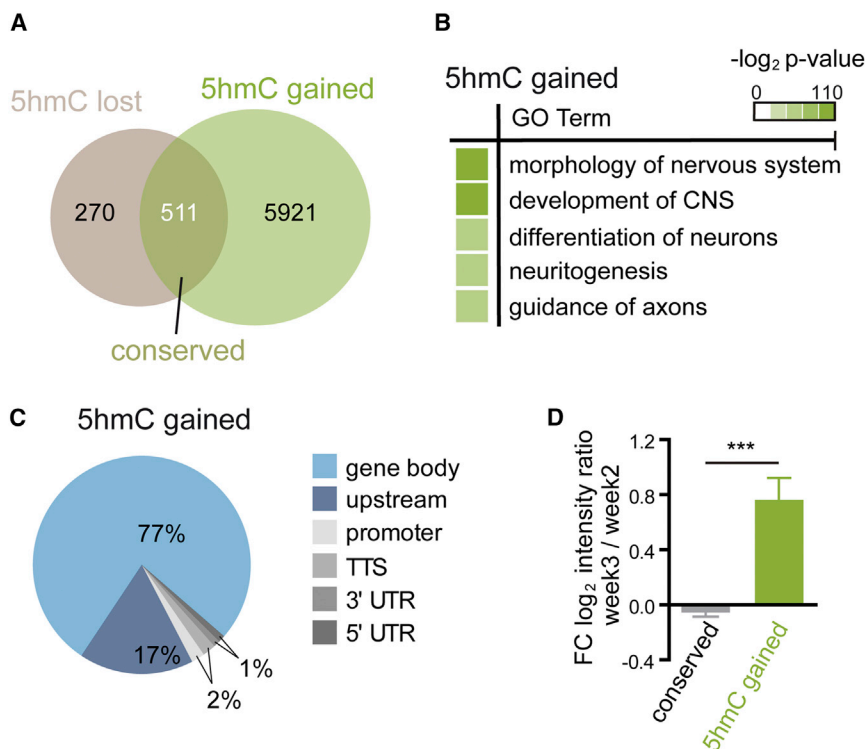


Figure 2. Genomic Localization of 5hmC in the Mouse Retina and Its Effect on Gene Expression

(A) Venn diagram shows 5hmC dynamics during retinal maturation (postnatal week 3/postnatal week 2).
 (B) GO analysis of genes that gained 5hmC during retinal maturation is shown.
 (C) Pie chart shows intragenomic distribution of 5hmC regions in mature retina.
 (D) LFQ of proteins encoded by genes with conserved (gray) or gained (green) 5hmC levels during retinal maturation. Summary data are mean \pm SEM. ***p < 0.001 (Student's t test). TSS, transcription starting site; TTS, transcription termination site. See also Figure S2 and Table S9.

unknown DNA-binding (transcription) factors could bind and target neuronal TET3 to pre-existing 5mC for subsequent oxidation to 5hmC (Figure 3C). To identify nuclear proteins that have the potential to specifically bind to neuronal TET3 in mouse retina, we combined affinity purification with mass spectrometry (MS). To this end, we transduced mouse retinal explant cultures with lentiviral vectors expressing an eGFP-fusion protein of the neuronal TET3 splice variant. Control cultures were transduced with lentiviral vectors expressing eGFP only. After onset of expression, nuclear protein complexes were extracted, affinity-purified, and subsequently labeled with TMT 2-plex reagents in forward and reverse label-swap experiments for comparative quantification using LC-MS (see the Experimental Procedures). These experiments allowed us to identify 52 proteins that were significantly enriched for binding to TET3 (>1.5-fold enrichment) in forward and reverse labeling experiments (Figure 3D, bottom right quadrant). Notably, nine of those proteins, such as REST, SUZ12, and CEP290, could be classified as regulators of transcription (Figure 3D; Table S2). Another six proteins are histone variants involved in chromatin modification, i.e., H3F3A and H2AFJ (Figure 3D; Table S2).

TET3 is endogenously expressed in the mouse retina (Figure 3A). Thus, TET3-eGFP is expected to compete for binding partners with endogenous TET3. To identify proteins that bind to endogenous TET3, we repeated the affinity purification experiment using a TET3-specific antibody. Endogenous TET3 was highly enriched by the antibody highlighting its specificity (Figure 3E). Moreover, we identified five transcriptional regulators (ASXL1, CTCF, MORF4L1, REST, and VAX1), three H3K36 methyltransferases (NSD2, NSD3, and SETD2), and histone 3 (H3F3A)

as interactors with significant enrichment for binding to endogenous TET3 (>1.5-fold) (Figure 3E; Table S3). Interestingly, the TET3-interacting protein with the highest enrichment score was the transcriptional repressor REST (Figure 3E), which was also significantly enriched in the TET3-eGFP affinity purification experiment (Figure 3D). To verify the TET3-REST interaction, we performed a reverse experiment using a REST-specific antibody that efficiently immunoprecipitates endogenous REST from mouse retina (Figure 3F; Table S4). Importantly, in this experiment, the REST antibody affinity-purified TET3 very efficiently with the overall third-highest enrichment score, but failed to immunoprecipitate TET1 and TET2 (Figure 3F). Moreover, none of the identified TET3 peptides was specific for the long CXXC-containing isoforms, suggesting that REST interacts specifically with the neuronal TET3 isoform. Taken together, these experiments identify REST as a major specific interacting protein of neuronal TET3.

REST Recruits Neuronal TET3 to Mediate 5hmC Formation and Transcriptional Activation

To determine the functional effects of REST on TET3 hydroxylase activity, we overexpressed TET3-eGFP alone and together with REST in HEK293T cells and subsequently quantified the 5hmC levels (Figure 4A). Non-transfected HEK293T cells have very low endogenous 5hmC levels, and overexpression of TET3-eGFP alone resulted in increased 5hmC levels (Figure 4A). Importantly, however, after co-expression with REST, TET3-eGFP generated significantly higher levels of 5hmC (Figure 4A). Conversely, after small interfering RNA (siRNA)-mediated knock-down of endogenous REST, overexpression of TET3-eGFP led to a significantly weaker elevation of 5hmC levels compared to control siRNA treatment (Figure 4B). Thus, REST is both necessary and sufficient to elevate TET3 hydroxylase activity.

REST is a transcriptional repressor that binds to specific RE-1 binding sites present in regulatory regions of its target genes (Kramer et al., 1992). Binding of REST results in transcriptional repression of the corresponding genes (Chong et al., 1995; Schoenherr

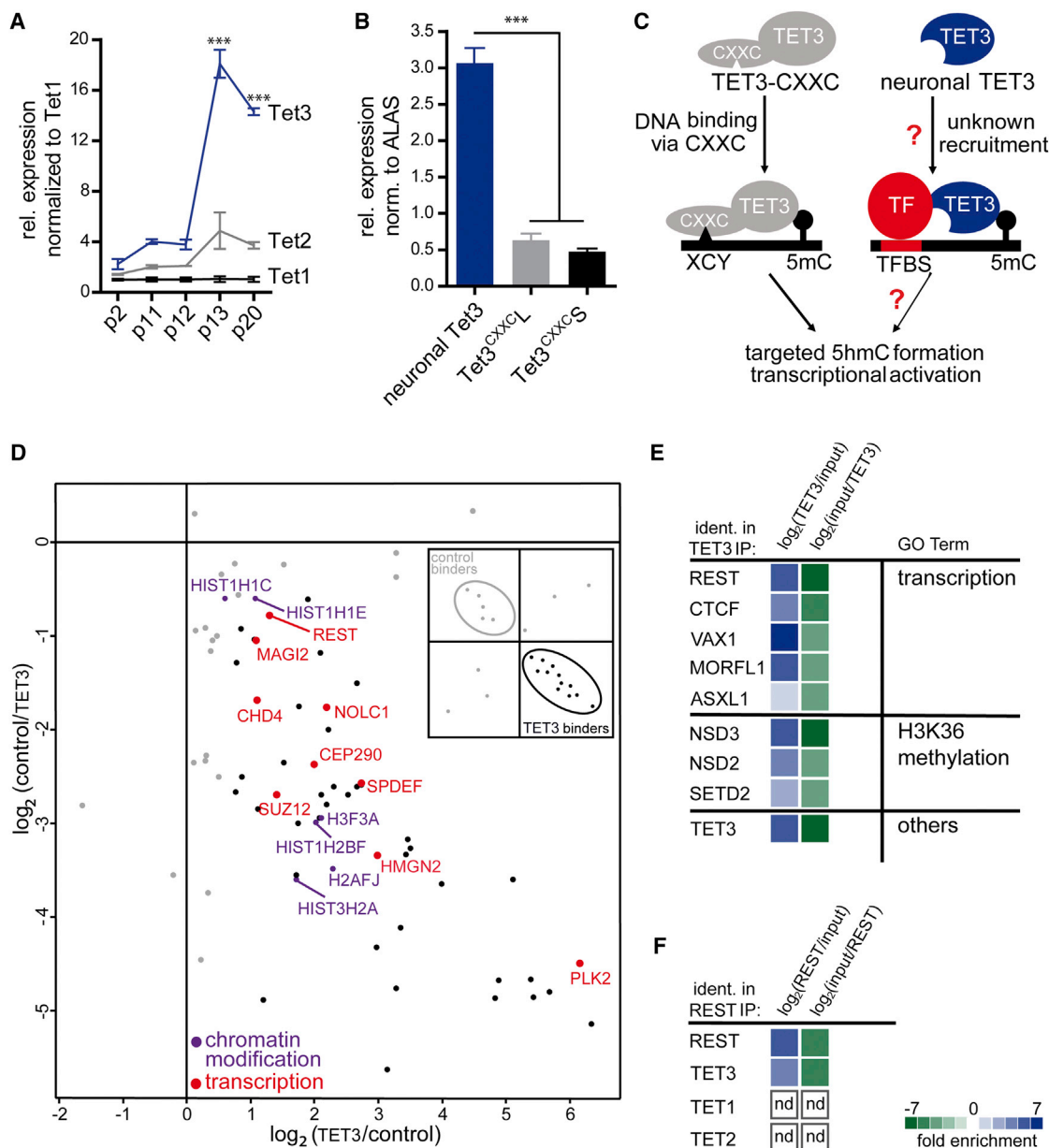


Figure 3. Tet Expression Levels and Identification of TET3-Interacting Proteins in Retina

(A) qRT-PCR analysis of Tet1, Tet2, and Tet3 gene expression in mouse retina at postnatal day (p) 2, 11, 12, 13, and 20 normalized to corresponding Tet1 levels. Tet3 is expressed significantly higher than Tet1 and Tet2 at p13 and p20.

(B) qRT-PCR analysis of Tet3 isoforms. Tet3 lacking a CXXC DNA-binding domain (neuronal Tet3) is the main isoform in retina.

(C) Cartoon illustrating putative DNA-binding mechanisms of TET3 isoforms lacking (neuronal TET3) or containing a CXXC domain. We hypothesized that neuronal TET3 is recruited to the DNA by transcription factors for context-specific hydroxymethylation and induction of gene expression.

(D) Scatter plot is shown of TET3 interactors identified using lentiviral TET3-eGFP overexpression (OE) in retinal explant cultures followed by GFP-trap and LC-MS/MS.

(E) Heatmap of endogenous TET3 interaction partners identified by immunoprecipitation and LC-MS/MS is shown.

(F) Heatmap of endogenous REST immunoprecipitation LC-MS/MS experiment confirms the interaction with endogenous TET3 (nd, not detected). Summary data are mean \pm SEM in (A and B). *** $p < 0.001$ (one-way ANOVA). See also Table S10.

and Anderson, 1995). We therefore asked whether TET3 might affect gene expression of REST target genes. To address this question, we overexpressed TET3-eGFP in HEK293T cells that endogenously contained REST (Dietrich et al., 2012), and we

determined the global protein levels using LFQ (Figures 4C–4E). Overexpression of TET3-eGFP resulted in significant upregulation of 40 proteins, and 26 of those were previously non-expressed (proteins with infinite log2 ratios in Figure 4E).

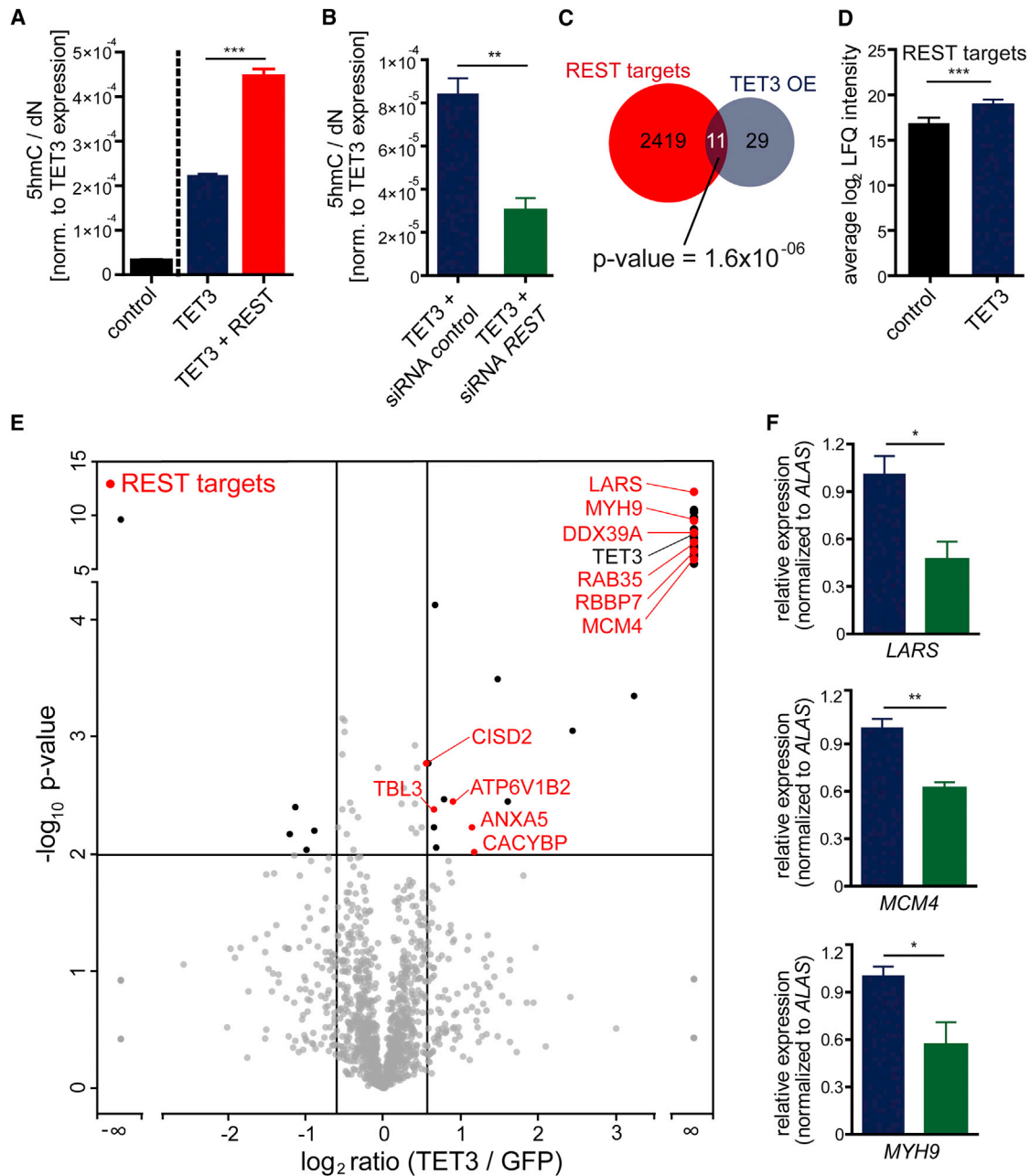


Figure 4. Functional Analysis of the Interaction of Transcriptional Repressor REST with Neuronal TET3

(A) UHPLC-MS/MS quantification of global 5hmC levels after OE of TET3-eGFP or REST and TET3-eGFP is shown.

(B) UHPLC-MS/MS quantification of global 5hmC levels after OE of TET3-eGFP in the presence of siRNA directed against human REST or a scrambled siRNA control (ctrl) is shown.

(C) Identification of global REST target gene expression using LFQ after eGFP (control) or TET3-eGFP OE in HEK293T cells. REST target genes are expressed significantly higher after TET3 OE.

(D) Venn diagram shows the significant overlap (Fisher's exact test; p value = 1.6×10^{-6}) of proteins enriched after TET3 OE and REST target genes in HEK293T cells.

(E) Volcano plot of protein expression ratios between TET3-eGFP and eGFP OE experiments in HEK293T cells as a function of statistical significance (Student's t test p value ≤ 0.01). Proteins with no statistically significant difference in expression between subsets are gray. Proteins with no detectable signal in one of the subsets were assigned a ratio of infinity. REST target genes are highlighted in red.

(F) Quantification of gene expression of three TET3-induced REST target genes in HEK293T cells using qRT-PCR after OE of TET3-eGFP in the presence of siRNA directed against human REST (green) or a scrambled siRNA control (ctrl, blue). Summary data in (A–C and F) are mean \pm SEM. *p < 0.05, **p < 0.005, ***p < 0.001 (Student's t test). See also Table S11.

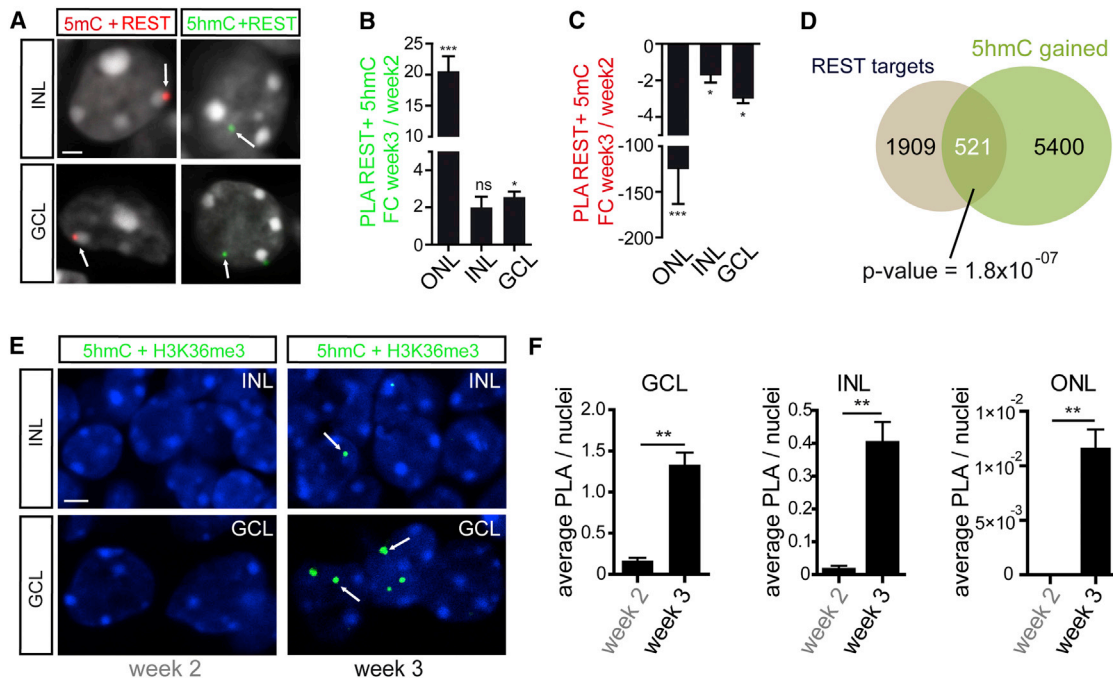


Figure 5. Accumulation of 5hmC in REST Target Genes Is Associated with Chromatin Remodeling

(A) PLA signal for 5mC and REST (red) is localized in heterochromatin. In contrast, the PLA signal for 5hmC and REST is localized in euchromatin (green). (B and C) Quantification data of the 5hmC/REST (B) and 5mC/REST (C) PLA experiments in (A) are shown. (D) Venn diagram shows the significant overlap (Fisher's exact test; p value = 1.8×10^{-07}) of REST target genes and 5hmC-gained genes during retinal maturation. (E) PLA signal for 5hmC and H3K36me3 (green) in nuclei of the INL (top) and the GCL (bottom) at week 2 (left) and week 3 (right). (F) Quantification data of the 5hmC/H3K36me3 PLA experiments in (E) are shown. Summary data in (B, C, and F) are mean \pm SEM. *p < 0.05, **p < 0.01, ***p < 0.001 (Student's t test). Scale bar, 1 μ m in (A) and 5 μ m in (E).

Interestingly, 308 of the identified proteins were known REST targets (Lu et al., 2014), and the average log₂ LFQ intensity of those REST targets was significantly higher after TET3 overexpression compared to the eGFP control (Figure 4C). Importantly, 11 of the 40 TET3-induced proteins (p = 1.6×10^{-6} , Fischer's exact test) were REST targets (Figure 4D; Table S5) and six of those (DDX39A, LARS, MCM4, MYH9, RAB35, and RBBP7) were previously non-expressed proteins (Figure 4E; Table S5).

To test if this TET3-mediated induction of REST target genes in HEK293T cells depends on REST, we overexpressed TET3-eGFP in the presence of REST-specific siRNA or scrambled control siRNA and measured the transcript levels of *LARS*, *MCM4*, and *MYH9* (Table S11). As shown in Figure 4E, all three REST target genes were exclusively expressed in the presence of TET3. Interestingly, in all three cases, the positive effect of TET3 on gene expression was significantly lower after knock-down of endogenous REST (Figure 4F), confirming that TET3 requires the presence of REST to de-repress REST target genes.

Accumulation of 5hmC in REST Target Genes Is Associated with Chromatin Remodeling

These results indicate that REST directs TET3 to repressed target genes and subsequent hydroxylation of pre-existing 5mC, then leads to de-repression and transcriptional activation of the genes. Repressed genes are usually found in hetero-

chromatin, whereas actively transcribed genes are located in euchromatin. As shown in Figure 1F, 5mC is enriched in heterochromatic structures and 5hmC in euchromatin. To test for the co-localization of REST with 5mC and 5hmC in nuclei of retinal neurons, we applied an in situ proximity ligation assay (PLA) combining REST-specific with 5mC- or 5hmC-specific antibodies. PLA gives only a positive signal when 5mC or 5hmC and REST are in close proximity (<40 nm) (Söderberg et al., 2006). We observed a positive PLA signal for both combinations, REST/5mC as well as REST/5hmC (Figure 5A). Importantly, the PLA signal for REST/5mC was localized in heterochromatin (Figure 5A, top), whereas the REST/5hmC signal was observed in euchromatin (Figure 5A, bottom). Thus REST-binding sites show distinct subnuclear localization depending on the oxidation status of adjacent genomic cytosines. Interestingly, the levels of PLA signal for REST/5mC and REST/5hmC varied significantly between week 2 and week 3 (Figures 5B and 5C). In particular, the REST/5hmC PLA signal correlated positively with the 5hmC levels increasing from week 2 to week 3 (Figure 5B). In contrast, the PLA signal for REST/5mC showed an inverse behavior, decreasing during the same period of time (Figure 5C). Together, these results suggest a functional correlation between REST-binding sites and proximal epigenetic DNA marks that might affect chromatin state and gene expression.

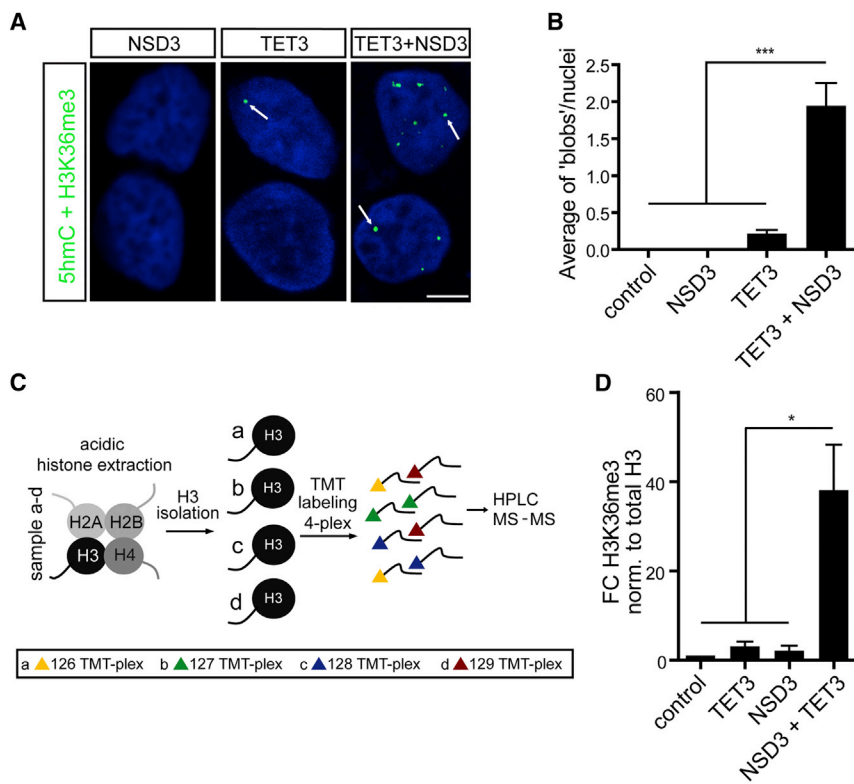


Figure 6. Effect of TET3-Mediated Hydroxylation on Chromatin Structure

(A) PLA signal for 5hmC and H3K36me3 in HEK293T cells overexpressing NSD3 (left), TET3-eGFP (middle) and TET3 + NSD3 (right).

(B) Quantification data of the 5hmC/H3K36me3 PLA experiments in (A) are shown.

(C) Scheme of TMT⁴-plex isobaric labeling and LC-MS quantification of H3 modifications is shown.

(D) Isobaric labeling LC-MS quantification of H3K36me3 in HEK293T cells overexpressing TET3, NSD3, or TET3 and NSD3 compared to non-transfected cells. Summary data are mean \pm SEM in (B and D). * $p < 0.05$, *** $p < 0.001$ (one-way ANOVA). Scale bar, 5 μ m in (A).

tone H3 at lysine 36 (H3K36), which is an epigenetic mark commonly associated with transcription of active chromatin (Bernstein et al., 2005; Heintzman et al., 2007; Kouzarides, 2007).

TET3 Regulates NSD3 H3K36 Trimethylation Activity

To test if the TET3/NSD3 interaction is functionally relevant, we performed a PLA experiment with HEK293T cells transfected with TET3 and/or NSD3,

focusing on the co-localization of the products of the two enzymes, 5hmC and H3K36me3, respectively. NSD3 overexpression did not result in any detectable PLA signal (Figures 6A and 6B), which is in line with the very low levels of 5hmC in HEK293T cells (see Figure 4A). TET3-overexpressing cells showed only a few PLA signals, indicating that 5hmC elevation alone does not automatically result in 5hmC/H3K36me3 co-localization (Figures 6A and 6B). However, when both TET3 and NSD3 were overexpressed, we observed a synergism that resulted in a significant increase of the 5hmC/H3K36me3 PLA signal (Figures 6A and 6B). We next isolated and enriched histone 3 and quantified the extent of K36 trimethylation of histone 3 using isobaric labeling and MS (Figure 6C). This experiment showed a 40-fold increase in the levels of H3K36me3 in the HEK293T cells co-overexpressing TET3 and NSD3 compared to non-transfected cells (Figure 6D). Overexpression of TET3 or NSD3 alone provided only about a 2-fold increase of the H3K36me3 activation mark (Figure 6D). Thus, TET3 has a synergistic effect on the lysine methyltransferase activity of NSD3.

TET3 Overexpression in Retina Leads to Neuronal Gene Activation and H3K36me3

To analyze if TET3 overexpression has an effect on global gene expression in the retina, we transduced retinal explant cultures with lentiviral vectors expressing TET3-eGFP. Compared to retinal explant cultures overexpressing eGFP only, we identified 981 proteins that were upregulated after TET3-eGFP overexpression (Table S6). The TET3-eGFP overexpression strongly affects gene expression in the retina, resulting in the upregulation of proteins involved in several neurological functions (Figure 7A).

To test if REST has an effect on the genomic 5hmC content in the retina, we re-analyzed our 5hmC mapping data (see Figures 2A–2C) by searching for known REST target genes (Lu et al., 2014) within the subset of genes that gained 5hmC marks from week 2 to week 3 (Figure 5D). In support of a positive effect of REST on genomic 5hmC levels in the retina, we found a significant enrichment of REST target genes within the group of genes that gained 5hmC during retinal maturation ($p = 1.8 \times 10^{-7}$, Fischer's exact test) (Figure 5D).

Transcriptional activation of previously silenced genes requires chromatin remodeling, e.g., a switch from a heterochromatic to a euchromatic state (Voss and Hager, 2014). It was suggested that REST-mediated chromatin remodeling involves changes of the activating histone mark lysine 36 trimethylation of the nucleosomal histone H3 (H3K36me3) (Zheng et al., 2009). To test for this chromatin remodeling during retinal maturation, we analyzed the co-localization of 5hmC with H3K36me3 using specific antibodies in combination with PLA. As shown in Figures 5E and 5F, we observed a clear increase of the PLA signal for 5hmC/H3K36me3 co-localization in nuclei of 3-week-old retina, whereas at 2 weeks only a few or no PLA signals were observed. This increase in 5hmC/H3K36me3 PLA signal was observed in nuclei of all three major retinal layers (Figure 5F). Thus, from week 2 to week 3, the chromatin structure in retinal nuclei changed in a way that led to co-localization of 5hmC with the active chromatin mark H3K36me3.

Notably, three of the identified TET3-interacting proteins were the post-SET domain containing histone-lysine N-methyltransferases NSD3, NSD2, and SETD2 (Figure 3E). These histone writers are involved in the (tri-) methylation of nucleosomal his-

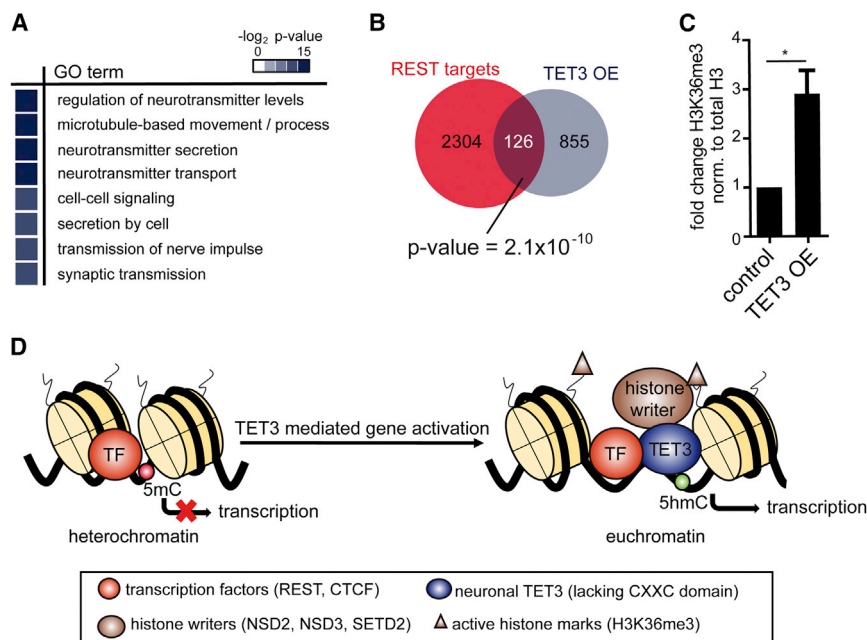


Figure 7. TET3 Overexpression Leads to Activation of Neuronal Genes and H3K36 Trimethylation during Retinal Maturation

(A) GO analysis reveals strong enrichment of neuronal proteins within the subset of proteins induced after TET3 OE in mouse retinal explants. (B) Venn diagram shows the significant overlap (Fisher's exact test; p value = 2.1×10^{-10}) of proteins enriched after TET3 OE and REST target genes.

(C) Isobaric labeling LC-MS quantification of H3K36me3 in mouse retina after TET3-eGFP or eGFP (control) OE. Summary data are mean \pm SEM. *p < 0.05 (Student's t test).

(D) Model for neuronal TET3-mediated transcriptional activation and chromatin remodeling. TET3 is recruited to the DNA by transcriptional regulators like REST for context-specific 5mC hydroxylation. Subsequently, TET3 mediates H3K36 trimethylation by recruitment of histone writers such as NSD3.

Correlation analysis again revealed that 126 known REST targets were significantly enriched in the subset of 981 TET3-upregulated proteins ($p = 2.1 \times 10^{-10}$, Fischer's exact test) (Figure 7B; Table S6).

To test whether TET3 also has a positive effect on lysine methyltransferase activity in the retina, we transduced retinal explant cultures with TET3-eGFP or eGFP using lentiviral vectors and determined the levels of H3K36me3 using isobaric labeling and MS. Overexpression of TET3-eGFP was able to elevate the levels of H3K36me3 by a factor of 3.8, suggesting that TET3-mediated hydroxylation of 5mC in retinal cells results in activation of NSD3 or similar enzymes to induce H3K36 trimethylation (Figure 7C). Our data indicate that this involves, at least in part, REST-assisted, TET3-mediated oxidation of genomic 5mC and subsequent NSD3-mediated chromatin remodeling.

DISCUSSION

Our comprehensive analysis of proteins interacting with the 5hmC-generating enzyme TET3 revealed a mechanism for specific epigenetic regulation of gene expression. We show that the transcription factor REST, a master regulator of genes involved in neuronal maturation processes (McGann et al., 2014), binds and recruits TET3 to the DNA for specific gene activation. In particular, we find that (1) REST regulates TET3 hydroxylase activity, (2) REST target genes accumulate 5hmC during retinal maturation, and (3) overexpression of TET3 activates REST target genes. In support of these findings, a recent study showed that deletion of REST in mouse embryonic stem cells (ESCs) led to significant loss of genome-wide 5hmC levels in regulatory regions (Feldmann et al., 2013). REST did not interact with TET1 or TET2. In addition, none of the TET3 peptides identified by MS after affinity purification of REST complexes from

mouse retinal lysates were specific for the TET3 isoforms with CXXC domain. Thus, REST-mediated recruitment of

TET3 seems to be specific for the neuronal TET3 isoform lacking a CXXC domain.

REST originally was described as a transcriptional repressor of neuronal genes in non-neuronal cells (Chong et al., 1995; Schoenherr and Anderson, 1995). In addition, REST was shown to be a key repressor in retinal ganglion cell commitment by preventing premature expression in retinal progenitor cells (Mao et al., 2011). It was hypothesized that, in neural progenitors, REST's repressive function is linked to gene regulatory networks related to neuronal differentiation (Mao et al., 2011). To act as a repressor, REST interacts with other proteins like mSin3a or COREST1 to form REST repressor complexes (Huang et al., 1999; McGann et al., 2014; Naruse et al., 1999). Importantly, none of the known REST-repressive complex proteins were identified in our REST-specific affinity purifications from mouse retinal lysates. There is now growing evidence suggesting that REST also plays a role in proper function of neuronal cells (Lu et al., 2014; Lunyak and Rosenfeld, 2005). For example, it was shown that REST functions as an activator of neuronal genes during neuronal maturation in the presence of a small double-stranded non-coding RNA corresponding to the NRSE/RE1 REST-binding sequence (Kuwabara et al., 2004).

Based on our 5hmC-mapping data, approximately 9% (521 of 5,921) of the genes that gained 5hmC during retinal maturation were known REST target genes. Thus, although REST contributes significantly ($p = 1.8 \times 10^{-7}$, Fischer's exact test) to context-dependent 5hmC generation, additional factors might exist for TET3 recruitment. In line with this, we identified several other transcriptional regulators interacting with TET3, such as ASXL1, CTCF, MORF4L1, SUZ12, and VAX1. It is tempting to speculate that these transcription regulators could influence TET3 hydroxylase activity in a similar way as REST. For instance, it was shown that the insulator CTCF interacts with TET enzymes

and that depletion of CTCF in mouse ESCs and adipocytes leads to significant loss of 5hmC in transcriptional enhancers (Dubois-Chevalier et al., 2014; Feldmann et al., 2013). However, CTCF seems not to discriminate among the TET isoforms, since it binds to TET1 and TET2 (Dubois-Chevalier et al., 2014) as well as to TET3 (present study).

Taken together, REST and most probably additional DNA-binding transcriptional regulators recruit TET3 to neuronal genes during retinal maturation to oxidize 5mC to 5hmC and activate their transcription. Transcriptional activation goes along with chromatin remodeling and translocation of genomic regions from 5mC-rich heterochromatin to 5hmC-rich euchromatin (Hahn et al., 2013; Mellén et al., 2012). Interestingly, our study reveals that TET3 interacts with several H3K36 methyltransferases. At a functional level TET3 stimulates the activity of NSD3 to generate the activating histone mark H3K36me3. Our data show that the transcriptional repressor REST can facilitate the recruitment of TET3 to 5mC-containing transcriptionally inactive genes (Figure 7D). This repressor-induced and context-specific recruitment is followed by TET3-mediated oxidation of 5mC to 5hmC. Subsequently, H3K36 methyltransferases induce chromatin remodeling to facilitate active transcription (Figure 7D).

Our findings favor a model that involves highly dynamic transcription-factor-dependent DNA hydroxymethylation that supports retinal network maturation by context-specific gene activation. Accordingly, our metabolic feeding experiments showed that the majority of nascent 5hmC marks were generated from pre-existing 5mC, supporting the idea of TET3-induced chromatin remodeling.

5hmC itself is known to recruit specific binding proteins (readers) (Mellén et al., 2012; Spruijt et al., 2013; Takai et al., 2014). We cannot exclude that such 5hmC readers might contribute to the observed TET3-mediated transcriptional activation during retinal maturation. Future study focusing on the identification of developmental-stage-specific 5hmC readers in the retina should help to elucidate their contribution.

In contrast to 5hmC, the levels of the further oxidized methylcytosine derivative 5fC in the retina were very low and decreased during neuronal maturation (see Figure S1C), suggesting that 5fC is a short-lived active DNA demethylation intermediate rather than an independent epigenetic mark in differentiating neuronal cells.

In conclusion, we provide evidence that TET3 and REST play a key role in the activation of neuronal gene transcription. Furthermore, we show that TET3-mediated gene activation involves H3K36 trimethylation-induced chromatin remodeling. This study provides a mechanistic link among REST-directed TET3-mediated 5hmC formation, subsequent chromatin remodeling by NSD3, and gene activation during neuronal maturation.

EXPERIMENTAL PROCEDURES

Animals

All mice used were on the C57BL/6 genetic background. All procedures concerning animals were performed with permission of the local authority (Regierung von Oberbayern). Day of birth was considered as postnatal day 1 (P1).

Lentiviral Constructs and Production

Mouse TET3 was PCR cloned from mouse retinal cDNA using the primers 5'-CTATCTAGAACCGCCATGGACTCAGGGCCAGTGAC-3' (forward) and 5'-TCACCGTAAGATCCAGCGGCTGTAGGG-3' (reverse), and ligated into a lentiviral vector containing a cytomegalovirus (CMV) promoter (Mistrík et al., 2005), yielding LV-CMV-TET3ΔCXXC-eGFP. LV-CMV-eGFP expressing eGFP only was used for control experiments. Recombinant lentivirus as well as lentiviral particles were generated as described previously (Mistrík et al., 2005).

In Vitro Retinal Explant Cultures

Retinas from wild-type animals were used to generate retinal explants. Animals were killed and the eyes enucleated in DMEM Nutrient Mixture F12-HAM medium (Sigma) containing 10% fetal bovine serum (FBS) and antibiotics. Afterward, the entire eyes were incubated in DMEM-F12 serum-free medium containing 0.12% proteinase K at 37°C for 15 min, to allow preparation of retinal cultures with RPE attached. Subsequently, proteinase K was inactivated using 10% FBS in DMEM Nutrient Mixture F12-HAM medium. The eyes were dissected aseptically in a Petri dish. The anterior segment, lens, vitreous, sclera, and choroids were carefully removed, and the retina was cut perpendicular to its edges, resulting in a cloverleaf-like shape. Subsequently, the retina was transferred to a Millicell culture dish filter insert (Millipore) with the retinal pigment epithelium layer facing the membrane. The insert was put into a six-well culture plate and incubated in DMEM-F12 Nutrient medium at 37°C.

Transduction of Retinal Explant Cultures

Retinal explant cultures from 11-day-old mice were used for transduction experiments using LV-CMV-TET3ΔCXXC-eGFP (neuronal TET3) or LV-CMV-eGFP (control). Twelve retinæ were used for each experiment. The LV particles were added to the scleral and vitreal part of retinal explants directly after preparation of the explant cultures. Every second day, the full volume of DMEM-F12, 1.2 ml per dish, was replaced with fresh medium. Retinal explants were harvested after 12 days in vitro for nuclear protein extraction.

Cell Culture and Transfection

HEK293T cells were grown at 37°C and 10% CO₂ in DMEM supplemented with 10% FBS, 100 units/ml penicillin, and 100 μg/ml streptomycin. The cells were transfected with plasmids expressing mouse REST (Addgene plasmid 21310) and/or mouse TET3 (LV-CMV-TET3ΔCXXC-eGFP, see above) using calcium phosphate. Cells were incubated at 37°C and 10% CO₂ for 48 hr, with an additional medium exchange step after 24 hr from transfection. Upon harvesting, the cells were washed once with PBS after removing the medium, pelleted, and then lysed for subsequent genomic DNA extraction as described below.

For RNAi experiments, REST-specific siRNA duplexes or control siRNA duplexes (OriGene, SR304036) and plasmid-expressing mouse TET3 were transfected using siTRAN (OriGene) in Opti-MEM I reduced serum medium (Invitrogen) according to the manufacturer's instructions. Cells were incubated at 37°C and 10% CO₂ for 48 hr and subsequently harvested for genomic DNA isolation. Knockdown efficiency of gene expression was verified using qRT-PCR.

Tracing Experiments with [¹³C,^D₃]-Labeled L-methionine in Retinal Explants

De novo methylation-tracing experiments with [methyl-¹³C,^D₃]-methionine were performed in p11 retinal explant cultures (as described in the Supplemental Experimental Procedures) that were maintained in methionine-free DMEM containing 10% FBS and supplemented with 2 mM [methyl-¹³C,^D₃]-methionine for 9 days (after 3 days, media were renewed). Four retinal cultures were collected each 3 days after feeding and pooled for subsequent UHPLC-MS/MS quantification.

Data Interpretation of Interactors

From the identified proteins, only the proteins that were enriched in both the forward and the reverse experiments, with an enrichment factor of at least 1.5-fold over the control sample, are claimed as interactors. GO analysis

was performed using Ingenuity pathway analysis (IPA, Ingenuity Systems, <http://www.ingenuity.com/>) or DAVID bioinformatics database (<http://david.abcc.ncifcrf.gov/>).

Acid Extraction of Histones

To examine histone modifications of histone 3 (H3), we followed a protocol from Shechter et al. (2007). In brief, cells were lysed in 1 ml hypotonic buffer containing 10 mM Tris-HCl (pH 8.0), 1 mM KCl, 1.5 mM MgCl₂, and 1 mM DTT. Samples were incubated for 30 min on rotator at 4°C. The intact nuclei were centrifuged at 10,000 × *g* for 10 min at 4°C. Next, the nuclei were re-suspended in 400 μl 0.4 N H₂SO₄ and samples were incubated on rotator for 30 min. The nuclear debris was removed by centrifugation at 16,000 × *g* for 10 min. The supernatant was incubated for 30 min with 132 μl trichloroacetic acid (TCA) to precipitate histones. Histones were pelleted by 16,000 × *g* for 10 min and washed with acetone without disturbing the pellet to remove remaining acid from the solution. The pellets were eluted using ddH₂O.

Quantification of Histone Modifications

The visible protein band of histone H3 was cut out of a Coomassie-stained SDS-gel after destaining. The protein was in-gel alkylated and tryptically digested (Shevchenko et al., 2006). Trypsin activity was stopped using 1 mM PMSF and the peptides were labeled according to manufacturer's protocol with the TMT 2 (retina) or the TMT 4 (HEK293T cells).

Post-labeled samples of each experiment were pooled together and analyzed via LC-MS/MS. The relative reporter ion intensities of the trimethylated H3K36 peptide were normalized to the relative quantities of the whole protein. Finally, the fold change of the trimethylated peptides was calculated in relation to each control sample.

Bioinformatics

Sequence reads of 5hmC containing DNA fragments were mapped onto the reference mouse genome (NCBI Build UCSC mm9) using the Bowtie (v0.12.7) algorithm. Unique and monoclonal reads were used for further analysis. Refseq genes were downloaded from the UCSC mm9 annotation database (UCSC Genome Browser). GO analyses on differentially hydroxymethylated regions were performed using Ingenuity (IPA, Ingenuity Systems).

ACCESSION NUMBERS

The NCBI GEO accession number for the 5hmC profiling data reported in this paper is GSE65860. The ProteomeXchange accession number for the proteomics data reported in this paper is PXD001857.

SUPPLEMENTAL INFORMATION

Supplemental Information includes Supplemental Experimental Procedures, two figures, and 11 tables and can be found with this article online at <http://dx.doi.org/10.1016/j.celrep.2015.03.020>.

AUTHOR CONTRIBUTIONS

S.M. and T.C. supervised the project. S.M., T.C., and A.P. designed experiments and interpreted data. A.P. conducted the analysis of gene expression, retinal explant culture, and LFQ proteomics. E.S., A.P., and N.M. performed protein pull-down studies. D.E. and S.K.L. performed peptide LC-MS quantification including sample preparation and analysis. A.F.K. conducted LFQ proteomics. M.W., J.S., and A.P. isolated genomic DNA. M.W., A.P., and J.S. performed sample preparation. M.W. and J.S. performed UHPLC-MS/MS quantification and isotope-tracing experiments of DNA bases. A.P., S.K., and S.M. performed and analyzed immunostainings and hMeDIP experiments. S.M. and E.S. generated expression plasmids and lentiviral vectors. A.P. and E.S. performed HEK293 cell culture experiments and acidic histone isolation. V.S. performed PLAs. A.P. and S.M. performed bioinformatics analysis. S.M. wrote the paper with input from other authors. M.B. and M.M. contributed to the experimental design, data interpretation, and manuscript editing.

ACKNOWLEDGMENTS

This work was supported by the Deutsche Forschungsgemeinschaft (DFG) cluster of excellence (CIPSM, EXC114). A.F.K. is supported by a fellowship from the Peter und Traudl Engelhorn-Stiftung. We thank Gail Mandel for the gift of anti-REST antibodies; Tim M. Strom and Thomas Meitinger for NGS; Lukas Windhager, Ralf Zimmer, and Michael Bonin for help with bioinformatics analysis; and Fred Koch for help with cloning and qPCR.

Received: November 7, 2014

Revised: January 9, 2015

Accepted: March 7, 2015

Published: April 2, 2015

REFERENCES

- Bernstein, B.E., Kamal, M., Lindblad-Toh, K., Bekiranov, S., Bailey, D.K., Huebert, D.J., McMahon, S., Karlsson, E.K., Kulbokas, E.J., 3rd, Gingeras, T.R., et al. (2005). Genomic maps and comparative analysis of histone modifications in human and mouse. *Cell* 120, 169–181.
- Chong, J.A., Tapia-Ramirez, J., Kim, S., Toledo-Aral, J.J., Zheng, Y., Boutros, M.C., Altshuler, Y.M., Frohman, M.A., Kraner, S.D., and Mandel, G. (1995). REST: a mammalian silencer protein that restricts sodium channel gene expression to neurons. *Cell* 80, 949–957.
- Colquitt, B.M., Allen, W.E., Barnea, G., and Lomvardas, S. (2013). Alteration of genic 5-hydroxymethylcytosine patterning in olfactory neurons correlates with changes in gene expression and cell identity. *Proc. Natl. Acad. Sci. USA* 110, 14682–14687.
- Dietrich, N., Lerdrup, M., Landt, E., Agrawal-Singh, S., Bak, M., Tommerup, N., Rappilber, J., Södersten, E., and Hansen, K. (2012). REST-mediated recruitment of polycomb repressor complexes in mammalian cells. *PLoS Genet.* 8, e1002494.
- Dubois-Chevalier, J., Oger, F., Dehondt, H., Firmin, F.F., Gheeraert, C., Staels, B., Lefebvre, P., and Eeckhoutte, J. (2014). A dynamic CTCF chromatin binding landscape promotes DNA hydroxymethylation and transcriptional induction of adipocyte differentiation. *Nucleic Acids Res.* 42, 10943–10959.
- Feldmann, A., Ivanek, R., Murr, R., Gaidatzis, D., Burger, L., and Schübeler, D. (2013). Transcription factor occupancy can mediate active turnover of DNA methylation at regulatory regions. *PLoS Genet.* 9, e1003994.
- Gregory-Evans, C.Y., Wallace, V.A., and Gregory-Evans, K. (2013). Gene networks: dissecting pathways in retinal development and disease. *Prog. Retin. Eye Res.* 33, 40–66.
- Hahn, M.A., Qiu, R., Wu, X., Li, A.X., Zhang, H., Wang, J., Jui, J., Jin, S.G., Jiang, Y., Pfeifer, G.P., and Lu, Q. (2013). Dynamics of 5-hydroxymethylcytosine and chromatin marks in Mammalian neurogenesis. *Cell Rep.* 3, 291–300.
- Heintzman, N.D., Stuart, R.K., Hon, G., Fu, Y., Ching, C.W., Hawkins, R.D., Barrera, L.O., Van Calcar, S., Qu, C., Ching, K.A., et al. (2007). Distinct and predictive chromatin signatures of transcriptional promoters and enhancers in the human genome. *Nat. Genet.* 39, 311–318.
- Hoon, M., Okawa, H., Della Santina, L., and Wong, R.O. (2014). Functional architecture of the retina: development and disease. *Prog. Retin. Eye Res.* 42, 44–84.
- Huang, Y., Myers, S.J., and Dingleline, R. (1999). Transcriptional repression by REST: recruitment of Sin3A and histone deacetylase to neuronal genes. *Nat. Neurosci.* 2, 867–872.
- Ko, M., An, J., Bandukwala, H.S., Chavez, L., Aijö, T., Pastor, W.A., Segal, M.F., Li, H., Koh, K.P., Lähdesmäki, H., et al. (2013). Modulation of TET2 expression and 5-methylcytosine oxidation by the CXXC domain protein IDAX. *Nature* 497, 122–126.
- Kouzarides, T. (2007). Chromatin modifications and their function. *Cell* 128, 693–705.
- Kraner, S.D., Chong, J.A., Tsay, H.J., and Mandel, G. (1992). Silencing the type II sodium channel gene: a model for neural-specific gene regulation. *Neuron* 9, 37–44.

- Kriaucionis, S., and Heintz, N. (2009). The nuclear DNA base 5-hydroxymethylcytosine is present in Purkinje neurons and the brain. *Science* 324, 929–930.
- Kuwabara, T., Hsieh, J., Nakashima, K., Taira, K., and Gage, F.H. (2004). A small modulatory dsRNA specifies the fate of adult neural stem cells. *Cell* 116, 779–793.
- Liu, N., Wang, M., Deng, W., Schmidt, C.S., Qin, W., Leonhardt, H., and Spada, F. (2013). Intrinsic and extrinsic connections of Tet3 dioxygenase with CXXC zinc finger modules. *PLoS ONE* 8, e62755.
- Lu, T., Aron, L., Zullo, J., Pan, Y., Kim, H., Chen, Y., Yang, T.H., Kim, H.M., Drake, D., Liu, X.S., et al. (2014). REST and stress resistance in ageing and Alzheimer's disease. *Nature* 507, 448–454.
- Lunyak, V.V., and Rosenfeld, M.G. (2005). No rest for REST: REST/NRSF regulation of neurogenesis. *Cell* 121, 499–501.
- Mao, C.A., Tsai, W.W., Cho, J.H., Pan, P., Barton, M.C., and Klein, W.H. (2011). Neuronal transcriptional repressor REST suppresses an Atoh7-independent program for initiating retinal ganglion cell development. *Dev. Biol.* 349, 90–99.
- McGann, J.C., Oyer, J.A., Garg, S., Yao, H., Liu, J., Feng, X., Liao, L., Yates, J.R., 3rd, and Mandel, G. (2014). Polycomb- and REST-associated histone deacetylases are independent pathways toward a mature neuronal phenotype. *eLife* 3, e04235.
- Mellén, M., Ayata, P., Dewell, S., Kriaucionis, S., and Heintz, N. (2012). MeCP2 binds to 5hmC enriched within active genes and accessible chromatin in the nervous system. *Cell* 151, 1417–1430.
- Mistrič, P., Mader, R., Michalakis, S., Weidinger, M., Pfeifer, A., and Biel, M. (2005). The murine HCN3 gene encodes a hyperpolarization-activated cation channel with slow kinetics and unique response to cyclic nucleotides. *J. Biol. Chem.* 280, 27056–27061.
- Münzel, M., Globisch, D., Brückl, T., Wagner, M., Welzmler, V., Michalakis, S., Müller, M., Biel, M., and Carell, T. (2010). Quantification of the sixth DNA base hydroxymethylcytosine in the brain. *Angew. Chem. Int. Ed. Engl.* 49, 5375–5377.
- Naruse, Y., Aoki, T., Kojima, T., and Mori, N. (1999). Neural restrictive silencer factor recruits mSin3 and histone deacetylase complex to repress neuron-specific target genes. *Proc. Natl. Acad. Sci. USA* 96, 13691–13696.
- Okawa, H., Hoon, M., Yoshimatsu, T., Della Santina, L., and Wong, R.O. (2014). Illuminating the multifaceted roles of neurotransmission in shaping neuronal circuitry. *Neuron* 83, 1303–1318.
- Santiago, M., Antunes, C., Guedes, M., Sousa, N., and Marques, C.J. (2014). TET enzymes and DNA hydroxymethylation in neural development and function - how critical are they? *Genomics* 104, 334–340.
- Schiesser, S., Pfaffeneder, T., Sadeghian, K., Hackner, B., Steigenberger, B., Schröder, A.S., Steinbacher, J., Kashiwazaki, G., Höfner, G., Wanner, K.T., et al. (2013). Deamination, oxidation, and C-C bond cleavage reactivity of 5-hydroxymethylcytosine, 5-formylcytosine, and 5-carboxycytosine. *J. Am. Chem. Soc.* 135, 14593–14599.
- Schoenherr, C.J., and Anderson, D.J. (1995). The neuron-restrictive silencer factor (NRSF): a coordinate repressor of multiple neuron-specific genes. *Science* 267, 1360–1363.
- Shechter, D., Dormann, H.L., Allis, C.D., and Hake, S.B. (2007). Extraction, purification and analysis of histones. *Nat. Protoc.* 2, 1445–1457.
- Shevchenko, A., Tomas, H., Havlis, J., Olsen, J.V., and Mann, M. (2006). In-gel digestion for mass spectrometric characterization of proteins and proteomes. *Nat. Protoc.* 1, 2856–2860.
- Söderberg, O., Gullberg, M., Jarvius, M., Ridderstråle, K., Leuchowius, K.J., Jarvius, J., Wester, K., Hydbring, P., Bahram, F., Larsson, L.G., and Landegren, U. (2006). Direct observation of individual endogenous protein complexes in situ by proximity ligation. *Nat. Methods* 3, 995–1000.
- Solovei, I., Kreysing, M., Lanctôt, C., Kösem, S., Peichl, L., Cremer, T., Guck, J., and Joffe, B. (2009). Nuclear architecture of rod photoreceptor cells adapts to vision in mammalian evolution. *Cell* 137, 356–368.
- Song, C.X., Szulwach, K.E., Fu, Y., Dai, Q., Yi, C., Li, X., Li, Y., Chen, C.H., Zhang, W., Jian, X., et al. (2011). Selective chemical labeling reveals the genome-wide distribution of 5-hydroxymethylcytosine. *Nat. Biotechnol.* 29, 68–72.
- Spruijt, C.G., Gnerlich, F., Smits, A.H., Pfaffeneder, T., Jansen, P.W., Bauer, C., Münzel, M., Wagner, M., Müller, M., Khan, F., et al. (2013). Dynamic readers for 5-(hydroxy)methylcytosine and its oxidized derivatives. *Cell* 152, 1146–1159.
- Szulwach, K.E., Li, X., Li, Y., Song, C.X., Wu, H., Dai, Q., Irier, H., Upadhyay, A.K., Gearing, M., Levey, A.I., et al. (2011). 5-hmC-mediated epigenetic dynamics during postnatal neurodevelopment and aging. *Nat. Neurosci.* 14, 1607–1616.
- Tahiliani, M., Koh, K.P., Shen, Y., Pastor, W.A., Bandukwala, H., Brudno, Y., Agarwal, S., Iyer, L.M., Liu, D.R., Aravind, L., and Rao, A. (2009). Conversion of 5-methylcytosine to 5-hydroxymethylcytosine in mammalian DNA by MLL partner TET1. *Science* 324, 930–935.
- Takai, H., Masuda, K., Sato, T., Sakaguchi, Y., Suzuki, T., Suzuki, T., Koyama-Nasu, R., Nasu-Nishimura, Y., Katou, Y., Ogawa, H., et al. (2014). 5-Hydroxymethylcytosine plays a critical role in glioblastomagenesis by recruiting the CHTOP-methylosome complex. *Cell Rep.* 9, 48–60.
- Voss, T.C., and Hager, G.L. (2014). Dynamic regulation of transcriptional states by chromatin and transcription factors. *Nat. Rev. Genet.* 15, 69–81.
- Williams, K., Christensen, J., Pedersen, M.T., Johansen, J.V., Cloos, P.A., Rappaport, J., and Helin, K. (2011). TET1 and hydroxymethylcytosine in transcription and DNA methylation fidelity. *Nature* 473, 343–348.
- Xiang, M. (2013). Intrinsic control of mammalian retinogenesis. *Cell. Mol. Life Sci.* 70, 2519–2532.
- Xu, Y., Wu, F., Tan, L., Kong, L., Xiong, L., Deng, J., Barbera, A.J., Zheng, L., Zhang, H., Huang, S., et al. (2011). Genome-wide regulation of 5hmC, 5mC, and gene expression by Tet1 hydroxylase in mouse embryonic stem cells. *Mol. Cell* 42, 451–464.
- Xu, Y., Xu, C., Kato, A., Tempel, W., Abreu, J.G., Bian, C., Hu, Y., Hu, D., Zhao, B., Cerovina, T., et al. (2012). Tet3 CXXC domain and dioxygenase activity cooperatively regulate key genes for *Xenopus* eye and neural development. *Cell* 151, 1200–1213.
- Zheng, D., Zhao, K., and Mehler, M.F. (2009). Profiling RE1/REST-mediated histone modifications in the human genome. *Genome Biol.* 10, R9.